# Modelling the effect of subcellular mutations on the migration of cells in the colorectal crypt

**CURRENT STATUS:** ACCEPTED

BMC Bioinformatics BMC Series

Lotte B Romijn
University of Melbourne

Axel A Almet
University of Oxford

Chin Wee Tan
Walter and Eliza Hall Institute

James Osborne
University Of Melbourne

jmosborne@unimelb.edu.au*Corresponding Author*
*ORCiD: https://orcid.org/0000-0002-5622-0104*

**DOI:**
10.21203/rs.2.10134/v1

**SUBJECT AREAS**
*Bioinformatics*

**KEYWORDS**
*Colorectal Cancer; Crypt; Multicellular Modelling; SBML; Chaste*

## Abstract

Background Many cancers arise from mutations in cells in epithelial tissues. Mutations manifesting at the subcellular level influence the structure and function of the tissue. In this paper we present a framework that allows the investigation of the influence of mutations such as subcellular knockouts and knockdowns on migration of cells within epithelial tissues.

Results In particular we investigate how specific mutations may lead to the increase in numbers of cells in the epithelial lining of the colorectal crypt, which may lead to the eventual destabilisation of the structure of the crypt and the onset of colorectal cancer. Secondly, we present the computational tools that allow the straightforward integration, and simulation of, SBML representations of subcellular dynamics with multicellular representations of the colorectal crypt.

Conclusions We see that mutations in APC can cause downward invasion of mutant cells in the crypt.

## Full-text

Due to technical limitations, full-text HTML conversion of this manuscript could not be completed.

However, the manuscript can be downloaded and accessed as a PDF.

## Figures

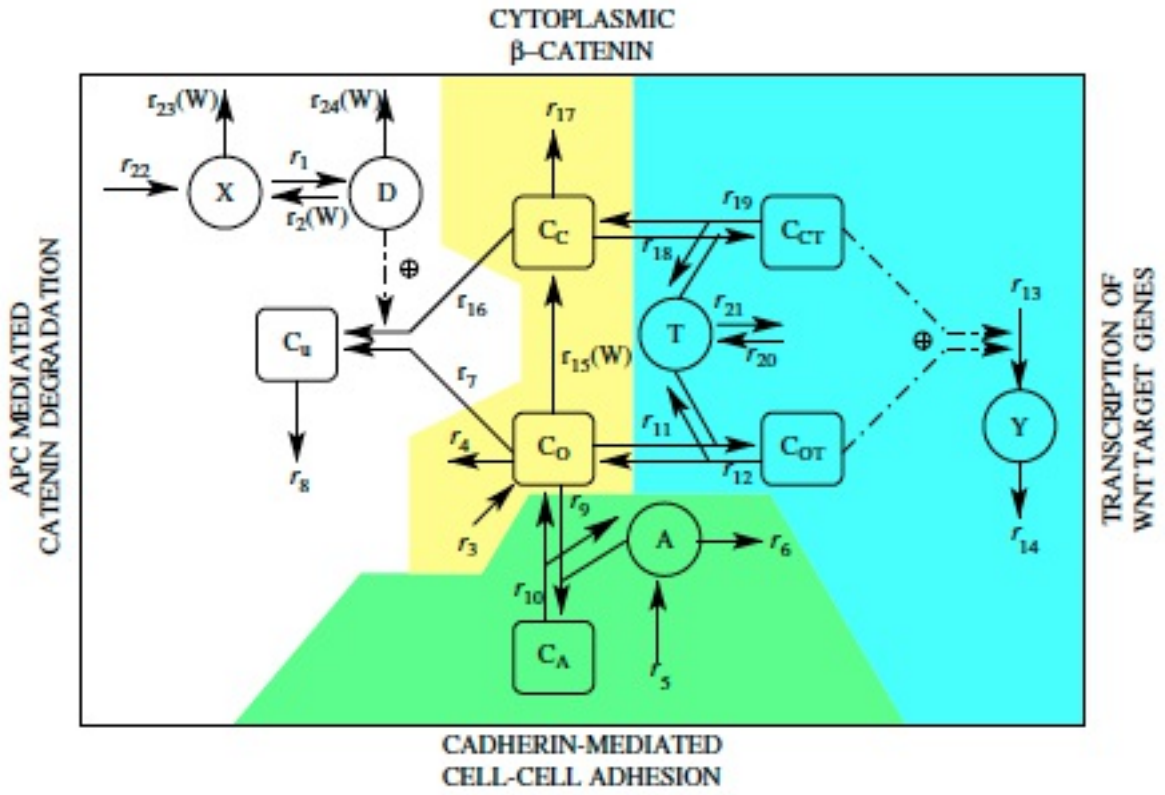


(a) VL

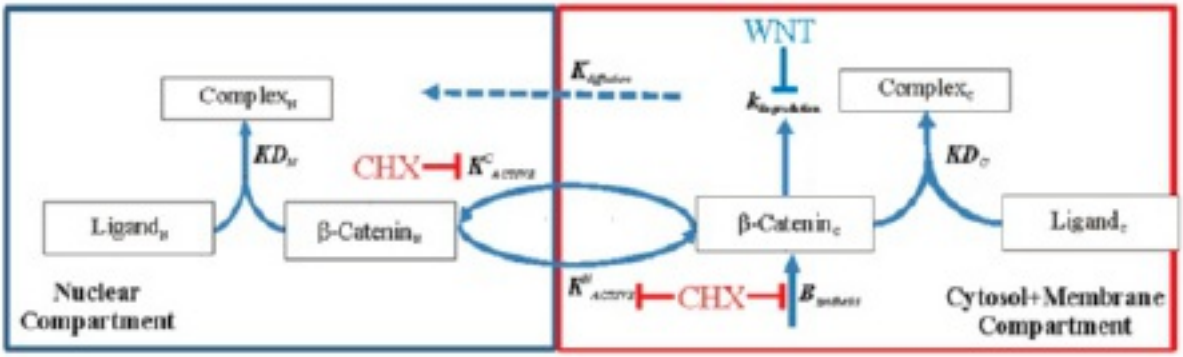


(b) Tan

Figure 1

Subcellular model schematics. a) Schematic representation of the VL model, which describes the dynamics of active destruction complexes (D), axin molecules (X), adhesion molecules (A), transcription molecules (T ), Wnt target proteins (Y ) and six pools of β-catenin (Ci, i = A, c, cT , o, oT and u). Reproduced with permission from [32]. b) Schematic representation of the Tan model which describes the dynamics of free and bound β-catenin in the cytosol-membrane (BC ,NC ) and nucleus (BN ,NN ), and free ligands in the cytosol-membrane (LC ) and nucleus (LN ). Reproduced with permission from [46].

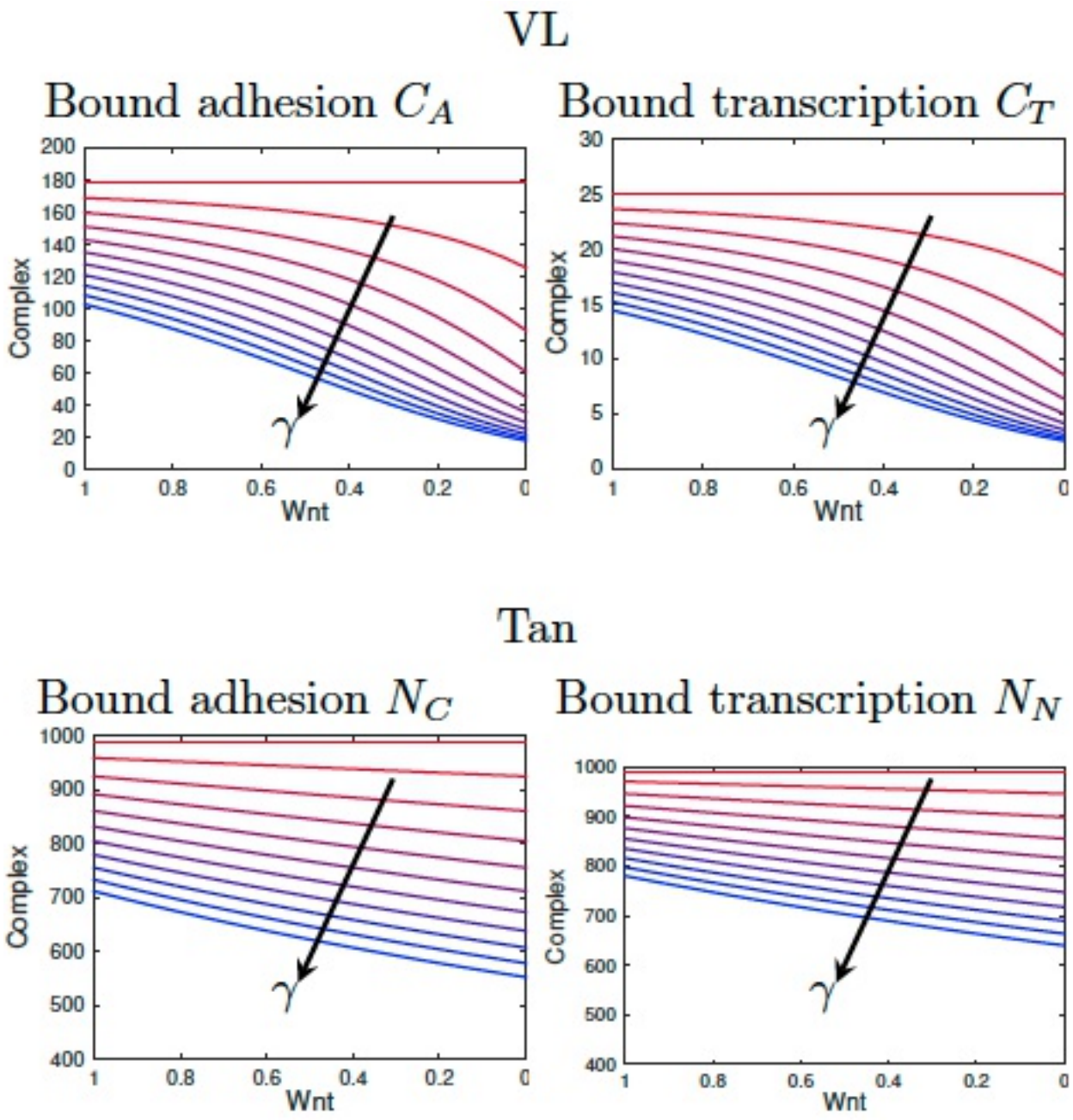


Figure 2

The effect of varying the expression of the APC mutation parameter, γ, on the bound complexes in the nucleus and cytosol-membrane. For the VL (top) and Tan models (bottom). Arrows are drawn in the direction of increasing γ. Decreasing γ increases the amount of bound complexes in both the complexes for adhesion and transcription. The cases are shown for $\gamma = 0 - 1$ in increments of 0.1 ($\gamma = 0$ is red, $\gamma = 1$ is blue).

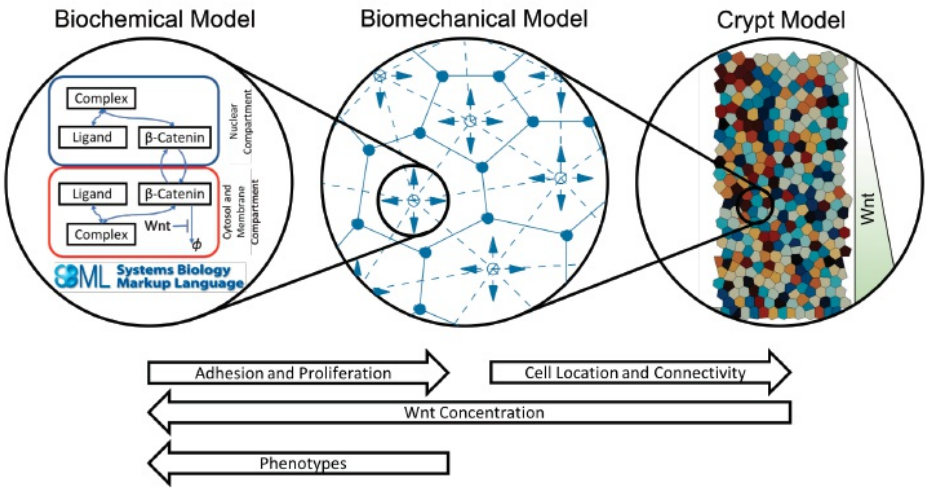


Figure 3

Schematic of the Model. The crypt model comprises a biomechanical model (the voronoi tessellation model found in Chaste) and a suitable biochemical model specied in SBML. The biochemical model species adhesion and cell proliferation in the biomechanical model which leads to cell movement in the crypt model. Cell phenotype (mutation level) and Wnt concentration are provided to the biochemical model by the biomechanical and crypt models respectively. SBML logo reproduced with permission from http://www.sbml.org.

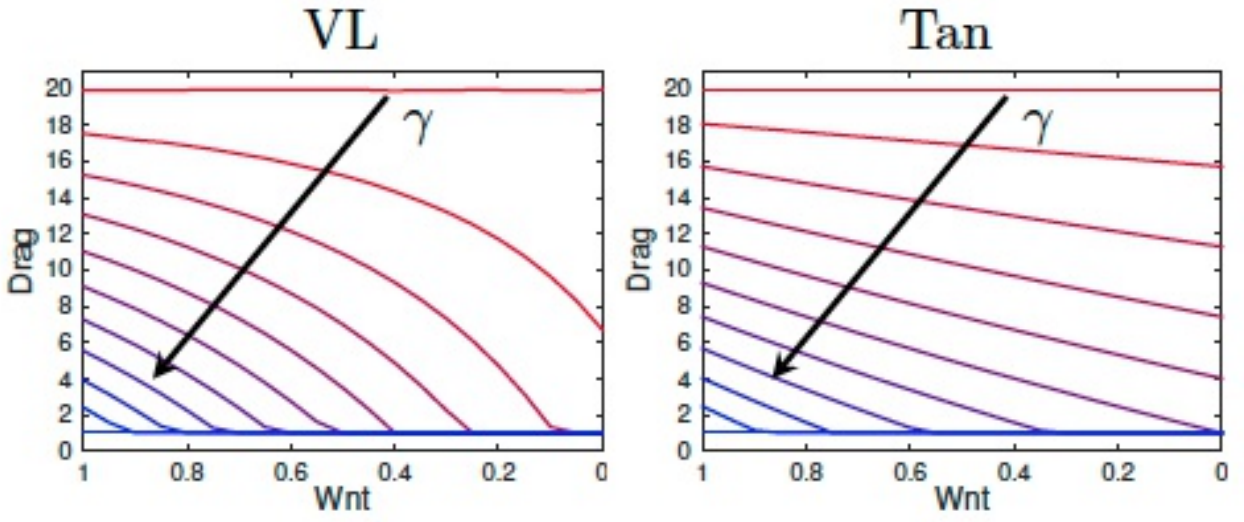


Figure 4

Drag functions: Drag as a function of the level of complex in the cytosol/membrane (CA in the VL model and NC in the Tan model). The lower , the higher the drag. I.e. for mutant cells the amount of complex in the cytosol/membrane increases, as seen in Figure 2, and we assume that this increases the drag. Also when the Wnt signal is higher, the drag will be higher for 6= 0 (as the amount of complex is higher). Arrows are drawn in the direction of increasing . The cases are shown for = 0 □ 1 in increments of 0.1 ( = 0 is red, = 1 is blue).

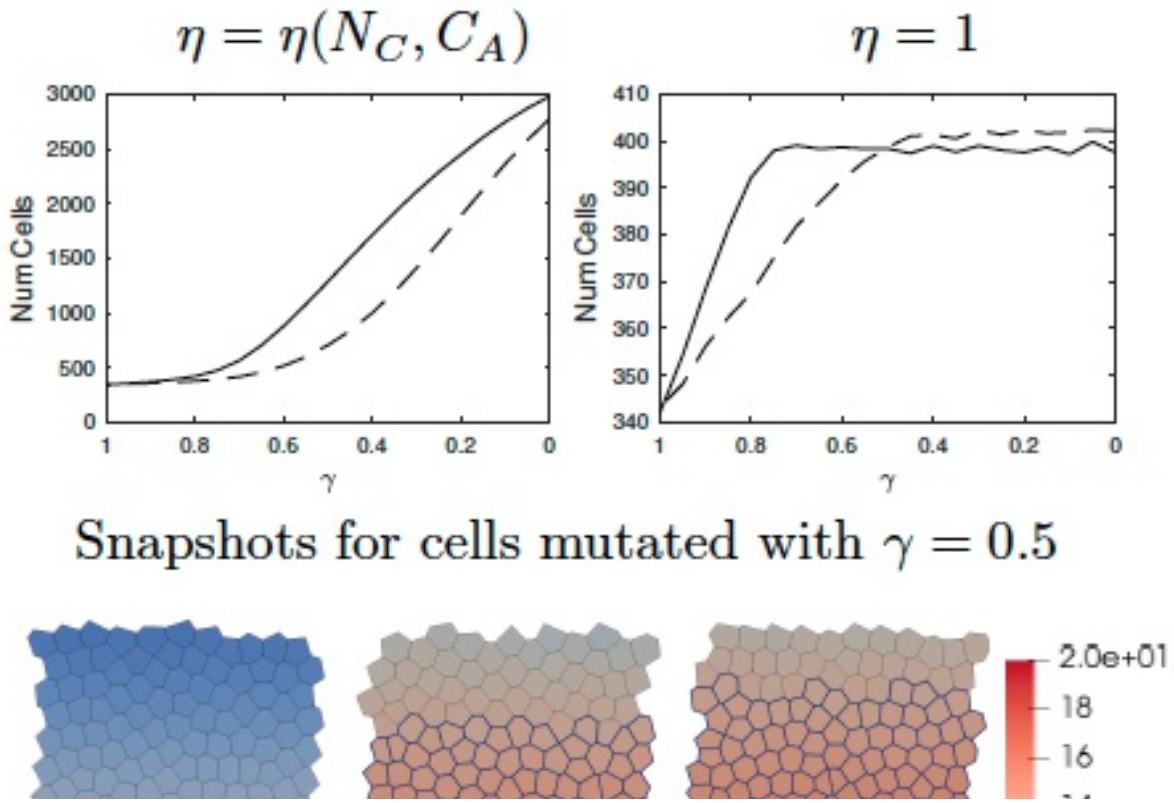

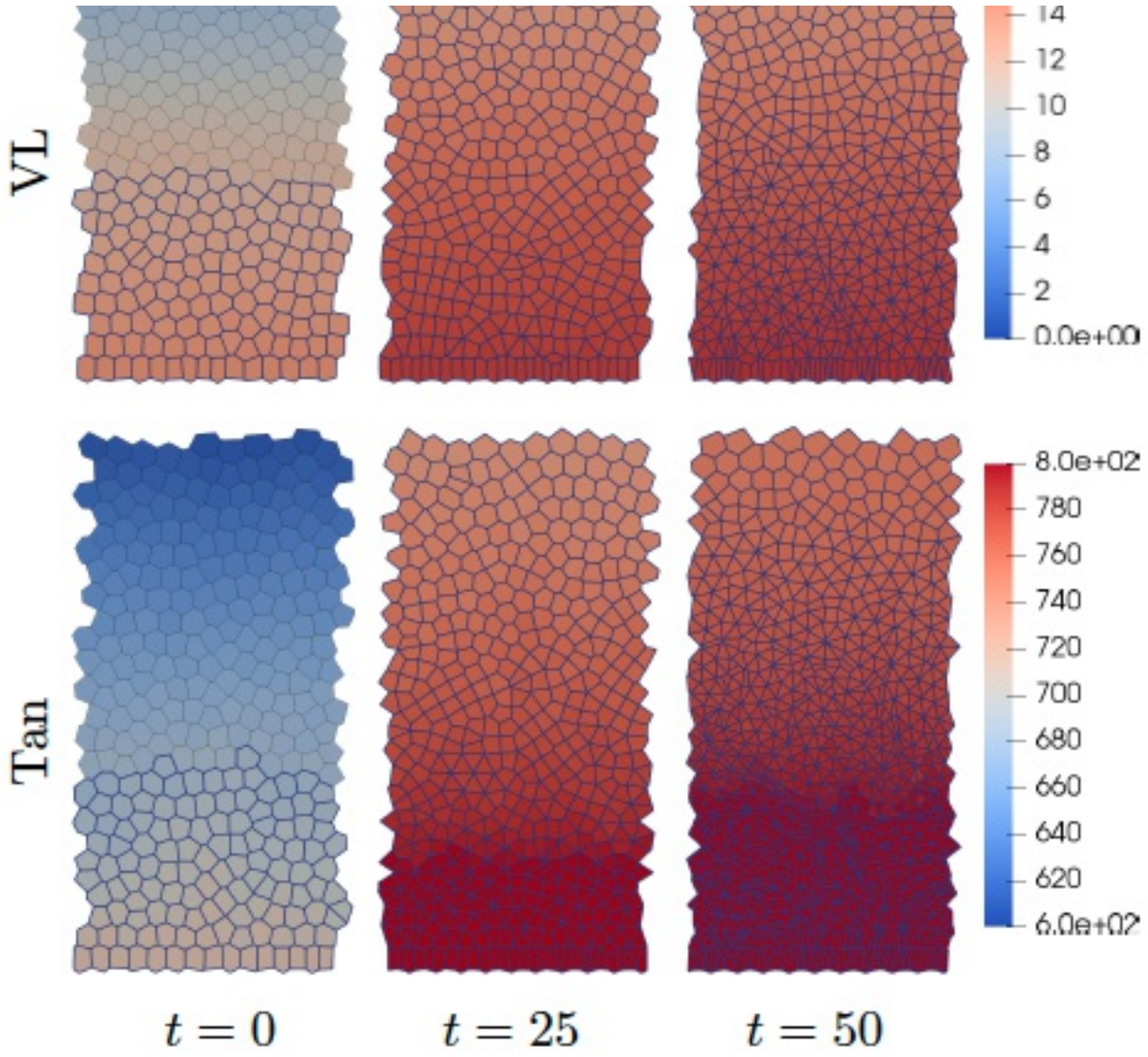


Figure 5

Number of cells in the crypt as a function of mutation parameter. Top) Averaged over 100 simulations for constant ( = 1) and variable drag (Equation (3)). All cells are mutated in a dynamic equilibrium, at time t = 0, the number of cells are counted at t = 50 hours. Dashed lines are with the VL model and solid line are with the Tan model. Bottom) Snapshots of simulations using the adhesion complex dependent drag functions dened in Equation (3). (random seed = 0). Proliferative cells are outlined in blue and cell color indicates level of nuclear complex. All cells in the crypts are mutated at time t = 0h, with parameter = 0:5, for both models.

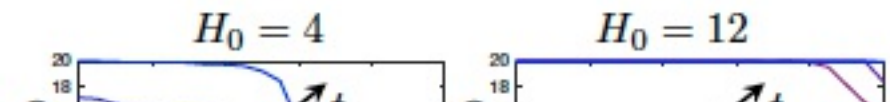

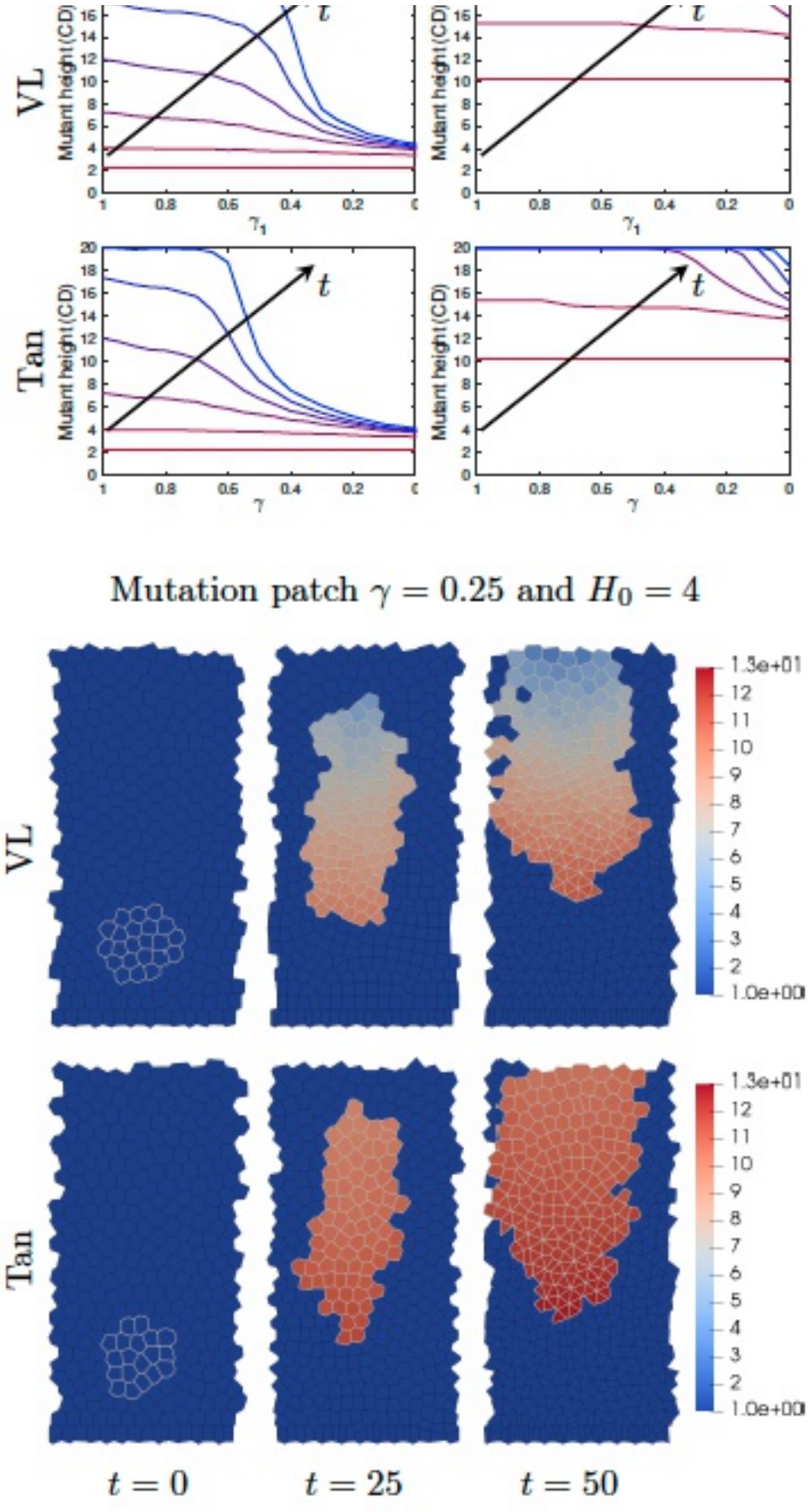
VL
Tan
Mutant height (CD)
$\gamma_1$
$\gamma$
$t$
Mutation patch $\gamma = 0.25$ and $H_0 = 4$
1.3e+01
1.0e+00
$t = 0$
$t = 25$
$t = 50$

Figure 6

Mutant cells remain in the crypt due to increased adhesion and proliferation. Top) Mutant height plotted at times t = 0, 10, 20, 30, 40, 50h after mutating cell. The simulations start with a mutant patch of radius 2, and initial centre height H0. The mutant height is given in cell diameters. Bottom) Snapshots of simulations with mutant cells at bottom of crypt, H0 = 4. (random seed =0). Mutated cells are outlined in grey and the cell color indicates level of drag coecient, , applied to the cell (function of adhesion complex). Mutant cells in the crypts are mutated at time t = 0h, with parameter = 0:25, for both models.

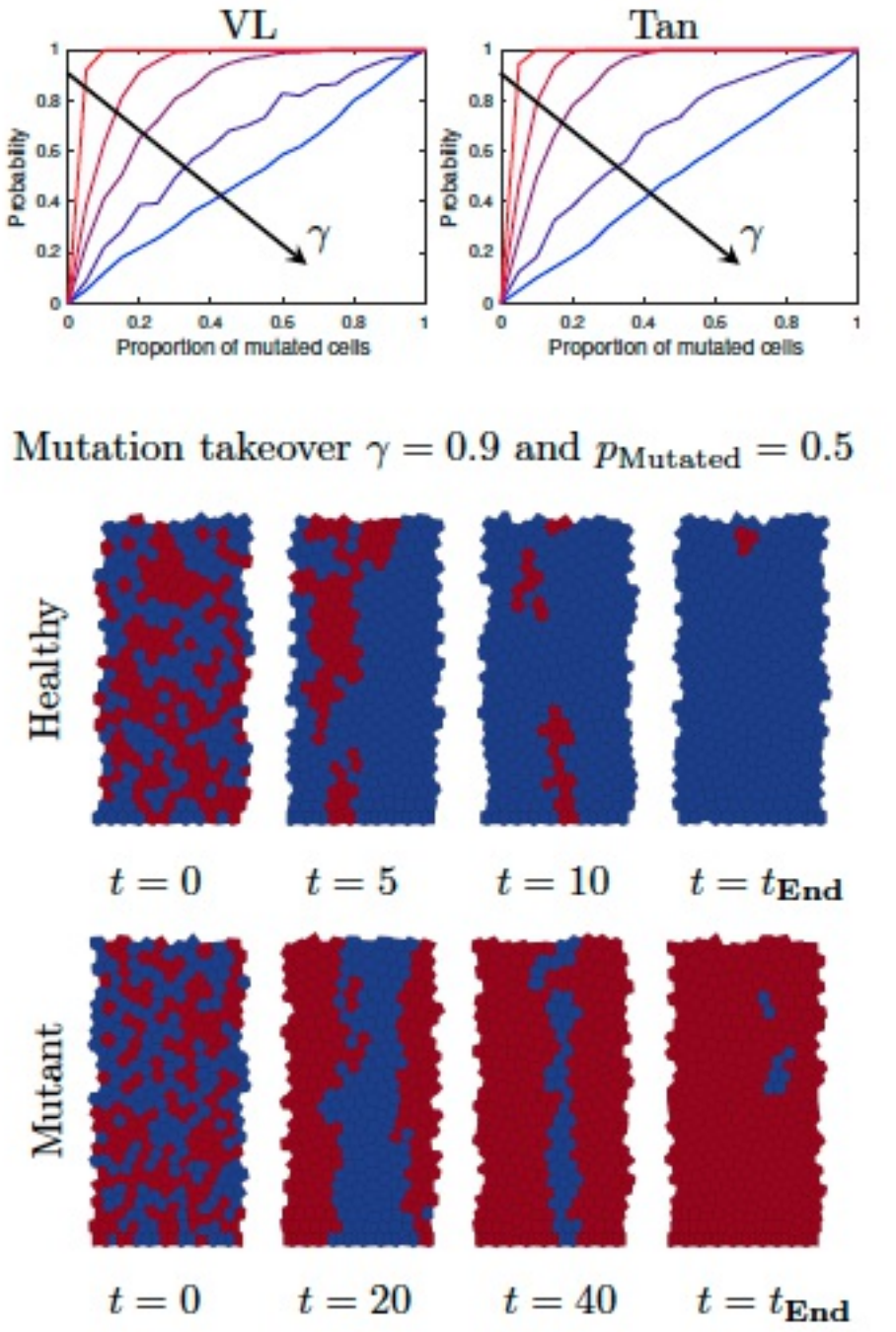


Figure 7

Mutant cells invade the crypt. Top) probability of mutant cells taking over the crypt as a function of initial proportion of mutated cells, for the VL and Tan models as the mutation parameter is varied. results are presented for = 0 (red); 0:5; 0:75; 0:9; and 1 (blue) and the arrow is in the direction of increasing Bottom) Snapshots of 2 simulations with 50% mutated cells. In the top simulation healthy cells happen to out compete the mutant cells, in the bottom simulation mutant cells win.